

Causal-discovery-based root-cause analysis and its application in time-series prediction error diagnosis

Hiroshi Yokoyama

HIROSHI-YOKOYAMA@BIWAKO.SHIGA-U.AC.JP

Faculty of Data Science, Shiga University / Division of Neural Dynamics, National Institute for Physiological Sciences / RIKEN AIP

Ryusei Shingaki

RYUSEI1.SHINGAKI@TOSHIBA.CO.JP

System AI Laboratory, Corporate Research & Development Center, Toshiba Corporation

Kaneharu Nishino

KANEHARU1.NISHINO@TOSHIBA.CO.JP

System AI Laboratory, Corporate Research & Development Center, Toshiba Corporation

Shohei Shimizu

SHOHEI-SHIMIZU@BIWAKO.SHIGA-U.AC.JP

Faculty of Data Science, Shiga University / RIKEN AIP

Thong Pham*

THONG-PHAM@BIWAKO.SHIGA-U.AC.JP

Faculty of Data Science, Shiga University / RIKEN AIP

Abstract

Recent rapid advancements of machine learning have greatly enhanced the accuracy of prediction models, but most models remain “black boxes”, making prediction error diagnosis challenging, especially with outliers. This lack of transparency hinders trust and reliability in industrial applications. Heuristic attribution methods, while helpful, often fail to capture true causal relationships, leading to inaccurate error attributions. Various root-cause analysis methods have been developed using Shapley values, yet they typically require predefined causal graphs, limiting their applicability for prediction errors in machine learning models. To address these limitations, we introduce the Causal-Discovery-based Root-Cause Analysis (CD-RCA) method that estimates causal relationships between the prediction error and the explanatory variables, without needing a pre-defined causal graph. By simulating synthetic error data, CD-RCA can identify variable contributions to outliers in prediction errors by Shapley values. Extensive simulations show CD-RCA outperforms current heuristic attribution methods, and a sensitivity analysis reveals new patterns where Shapley values may misattribute errors, paving the way for more accurate error attribution methods.

Keywords: Causal discovery, Shapley value (SV), Root-cause analysis (RCA), anomaly attribution, eXplainable AI (XAI), trustworthy AI (TAI)

1. Introduction

With the recent development of artificial intelligence (AI) technology based on various machine learning (ML) architectures, the predictive capability of ML methods has drastically improved. While applying ML-based prediction techniques in an industrial situation has attracted growing attention, the prediction mechanisms in most modern ML architectures (e.g., deep neural networks) are close to black box systems (Guidotti et al., 2018; Buhrmester et al., 2021). When there is something unexpectedly happened that lead to an unusually bad performance of the ML system, i.e., an outlier in the prediction error, the diagnosis of the reason for this outlier, e.g., how much each explanatory variable contributed to the outlieriness, is of paramount importance. It might not only lead

* corresponding author

to preventions of future catastrophic outliers, but also provide clues to improve the overall reliability, safeness, and trustworthiness of the ML system (Chamola et al., 2023; Li et al., 2023). However, the black-box nature of most modern ML architectures makes the diagnosis not straightforward, and in some cases near impossible, to perform manually by a human. Therefore, establishing an explainable AI (XAI) method to automatically diagnose outliers in prediction errors would be crucial to improve the development of AI applications for practical and industrial situations (Kaur et al., 2022; Hassija et al., 2023). However, current methods for understanding the root cause of outliers in prediction errors is still lacking.

In the context of XAI studies, various heuristic analysis methods for detecting the attributive variables in ML models for prediction error have been proposed (Ribeiro et al., 2016; Idé et al., 2021; Deng et al., 2021; Zhou et al., 2021; Idé and Abe, 2023; Deng et al., 2024). However, since these methods do not consider the causal relationships between the prediction error, the target variable, and the explanatory variables in the ML method, existing heuristic attribution methods do not necessarily reflect the causality in the generating process of the prediction error (Huang and Marques-Silva, 2024; Ma and Tourani, 2020), and thus might lead to erroneous attributions, as will be shown in Fig. 1.

Recently, root-cause analysis (RCA) that utilizes causality through various variants of the Shapley values (SV) (Shapley, 1953) have been extensively studied, with various methods proposed (Heskes et al., 2020; Jung et al., 2022; Budhathoki et al., 2022; Janzing et al., 2024). However, these methods are focused on the RCA of abrupt changes in target observations, rather than that of the prediction error from some black-box prediction model. Furthermore, to directly apply these methods to the attribution problem of prediction errors, one needs a causal graph that represents the causal relationships between the explanatory variable, the target variable, and the prediction error. Since the estimation of such a causal graph has not been considered in those works, it remains unclear whether these methods can be applied in XAI.

To address the above issues, we propose Causal-Discovery-based Root-Cause Analysis (CD-RCA), a novel XAI method that directly considers the causal processes behind prediction errors in machine learning-based methods. The key idea in our approach is to approximate the unobtainable causal relationships between the explanatory variables, the target variable, and the prediction error of a black-box prediction model f with a tractable causal structural model. This surrogate model allows us to generate synthetic samples of the prediction errors that approximately preserve the causality in the actual generating process of the observed prediction errors. This allows us to ask what would the prediction error look like if an explanatory variable X_p had followed its normal causal mechanism? Roughly speaking, such a counterfactual prediction error can be approximately generated from the surrogate causal model by randomizing the exogenous noise at X_p . Comparing this counterfactual prediction error with the actual outlier prediction error would give us an idea about the contribution of X_p . Specifically, the attribution of each variable to an outlier of the prediction error can be quantified by employing a version of the Shapley values, proposed by Budhathoki et al. (2022). At a high level, our main contributions are:

- We propose the CD-RCA method for model-agnostic prediction error attribution, and provide an adaptation of the method to time-series data. Our method is an extension of Budhathoki et al. (2022), in the sense that, unlike their method that require a known causal graph, our method does not assume any causal graph is known, and proceeds to estimate the causal graph between the explanatory variables, the target variable, and the prediction error. We show

through extensive simulations that CD-RCA outperforms existing methods in identifying the root cause of outliers in prediction errors.

- Through sensitivity analysis, we identified various previously-unknown patterns in which the Shapley values might fail to capture the correct attributions. Namely, CD-RCA might encounter difficulties in detecting the root cause variable when: (1) the amplitude of the anomalous noise is less than the mean of the exogenous noise, or (2) there is no causal effect of the root cause variable on the target variable. These results might have independent interests, as they provide clues for investigating other attribution methods that incorporate variants of the Shapley values.

The organization of the paper is as follows. We introduce our proposed method in Section 2. We provide an illustrative example to showcase its working in Section 3.1, and show the sensitivity analysis results in Sections 3.2, 3.3, and 3.4. Concluding remarks are given in Section 4. The programming code used to reconstruct all the results in this paper was implemented using the language Python, and can be found in the Supplementary materials.

2. Root-cause analysis of prediction error outliers

Suppose that we observe n samples from the joint distribution of the target variable Y , the covariates X_1, \dots, X_d , and the prediction error $r = Y - \hat{Y}$, where \hat{Y} is obtained from from some black-box prediction model. Denote these samples as $D_{\text{train}} = (X_{i,1}, \dots, X_{i,d}, Y_i, r_i)_{i=1}^n$. Assume that we want to use D_{train} to learn a model to measure the outlieriness of r^* in some target sample $((x_p^*)_{p=1}^d, y^*, r^*)$ from the joint distribution of (X_1, \dots, X_d, Y, r) . Note that this sample is not necessarily included in D_{train} . We also want to quantify the contribution of each X_p ($p = 1, \dots, d$) and Y to the outlieriness of r^* . To streamline the notation, we will sometimes use X_{d+1} , $X_{i,d+1}$, and x_{d+1}^* in place of Y , Y_i , and y^* , respectively, and X_{d+2} , $X_{i,d+2}$, and x_{d+2}^* in place of r , r_i , and r^* , respectively. We discuss how to measure the outlieriness of r^* in Section 2.1, and a general framework to define and calculate the attribution $\phi(p)$ of each X_p to this outlieriness in Section 2.2. In Section 2.3, we adapt this framework to time-series data. In Section 2.4, we discuss some modelling and computational aspects of our framework.

2.1. Outlier scores

For measuring the outlieriness of r^* , we use the following information-theoretic score $S(r^*)$ (Budhathoki et al., 2022).

$$S(r^*) = -\log \mathbb{P}\{\tau(r) \geq \tau(r^*)\}, \quad (1)$$

where $\tau : \mathbb{R} \rightarrow \mathbb{R}$ is some transformation. The outlier score $S(r^*)$ can be calculated, for example, by using the empirical distribution $(r_i)_{i=1}^n$ of r . This outlier score includes the familiar z -score when $\tau(r) = |r - \mu_r|/\sigma_r$ with μ_r and σ_r being the mean and standard deviation of the distribution of r , respectively.

This outlier score measures the outlieriness of the value r^* by the probability of the event $\tau(r) \geq \tau(r^*)$. When this probability is small, which means that the event is rare, the outlier score will be large. For example, considering the transformation $\tau(r) = |r - \mu_r|/\sigma_r$, a r^* that is unusually large when taken into accounts the mean and the variance of the distribution will give a large value of $\tau(r^*)$, thus leads to a large $S(r^*)$. Such an outlier r^* can be caused by either outlier values in one

or multiple covariates in X_1, \dots, X_d , and/or by an outlier value of the target variable Y . In the next section, we aim to *quantify the contribution* $\phi(p)$ of X_p to the outlier score $S(r^*)$, in such a way that reflects *the degree of causation* (Halpern and Hitchcock, 2015): the more X_p causes the outlier r^* , the larger the value of $\phi(p)$ should be.

2.2. The general framework

At the core of our framework is the approximation of the unattainable causal relationships between the variables X_1, \dots, X_d, Y and r by the following tractable surrogate causal model, which is known as additive noise models in the causality literature (Hoyer et al., 2008):

$$X_p = g_p((X_q)_{q \in pa(p)}) + N_p, \quad p = 1, \dots, d + 2, \quad (2)$$

where $pa(p)$ is the index set of the parents of X_p , and N_p is the exogenous noise random variable at X_p .

We build this surrogate causal model in three sub-steps. Firstly, we learn a causal graph G between (X_1, \dots, X_d, Y, r) by some causal discovery algorithm from the observational data. Secondly, we learn a parametric model g_p for each variable X_p , conditioning on its parents $pa(p)$. Based on the fitted values of the model, we then calculate the observed noise value of each variable for each sample: $n_{i,p} = X_{i,p} - \widehat{X}_{i,p}$ for $p = 1, \dots, d + 2$ and $i = 1, \dots, n$. Finally, we fit a parametric distribution for N_p based on the samples $n_{i,p}$. For an exogenous variable X_p whose parent set $pa(p)$ is empty, we fit a parametric distribution directly on $X_{i,p}$. By simulating a noise vector $(N_p)_{p=1}^{d+2}$ from the learned noise distributions, one can generate a sample (X_1, \dots, X_d, Y, r) using Eq. (2). The noises in the target sample $(y^*, (x_p^*)_{p=1}^d, r^*)$ can also be calculated from the causal graph and the learned model. In particular, the noise at X_p in the target sample is

$$n_p^* = x_p^* - g_p((x_q^*)_{q \in pa(p)}), \quad p = 1, \dots, d + 2, \quad (3)$$

where $g_p((x_q^*)_{q \in pa(p)}) = 0$ if $pa(p) = \emptyset$.

To calculate the attributions of each variable to $S(r^*)$, we employ the Shapley values proposed by Budhathoki et al. (2022). Denote $S(r^* | U)$ the counterfactual outlier score of r^* calculated from simulated data in which the noise value of a variable X_q with $q \notin U$ is fixed at its observed value n_q^* in the target sample, while we randomize the noise N_k of X_k for $k \in U$. This randomization can be done by sampling from the joint empirical distribution or the learned joint parametric noise distribution of $(N_k)_{k \in U}$. The value of $S(r^* | U)$ is counterfactual in the sense that it is the hypothetical value of $S(r^*)$ had the noises of the variables in U been randomized, i.e., not at their observed values in the target sample. Thus, the randomization has a whitening effect: the contributions of the variables $(X_k)_{k \in U}$ to the outlieriness of r^* has been whitened out in $S(r^* | U)$.

Suppose that we have already randomized the noise values of variables in some conditioning set $I \subseteq \{1, \dots, d + 2\} \setminus \{p\}$. This means that the contributions of the variables $(X_k)_{k \in I}$ to $S(r^*)$ have been whitened out. The change in the outlieriness of r^* when we further randomize N_p comparing with the current baseline outlieriness of r_i , i.e., the difference

$$\phi(p|I) = S(r^* | I \cup \{p\}) - S(r^* | I), \quad (4)$$

expresses the contribution of X_p to $S(r^*)$ when the contributions of $(X_k)_{k \in I}$ have been whitened out. Thus, $\phi(p|I)$ untangles the contribution of X_p from the contributions of $(X_k)_{k \in I}$.

Since this contribution depends on the conditioning set I , one can remove this dependency by defining the final, unconditional attribution of X_p as a weighted average of all $\phi(p|I)$:

$$\phi(p) = \sum_{I \subseteq \{1, \dots, d+2\} \setminus \{p\}} w_I \phi(p|I), \quad (5)$$

where $w_I = (d+2)^{-1} \binom{d+1}{|I|}^{-1}$ and $\sum_{I \subseteq \{1, \dots, d+2\} \setminus \{p\}} w_I = 1$.

This particular choice of the weights makes $\phi(p)$ precisely a Shapley value (Shapley, 1953), and thus the attribution $\phi(p)$ possesses some desirable properties from a game-theoretic perspective, including the following *efficiency property*:

$$S(r_i) = \sum_{p=1}^{d+2} \phi(p). \quad (6)$$

Note that this set of weights is the *unique* set that can achieve efficiency (under the presence of some other desirable properties) (Grabisch and Roubens, 1999). We summarize our framework in Algorithm 1. See Appendix A for a discussion on related works.

Algorithm 1 Causal-Discovery-based Root-Cause Analysis (CD-RCA)

Input: Training data $D_{\text{train}} = (X_{i,1}, \dots, X_{i,d}, Y_i, r_i)_{i=1}^n$, target outlier sample $((x_p^*)_{p=1}^d, y^*, r^*)$, a transformation τ

Output: Outlier score $S(r^*)$, attributions $(\phi(p))_{p=1}^{d+2}$

- 1 Estimate a causal graph G from D_{train}
 - 2 Learn parametric models for g_p and the distributions of N_p in Eq. (2)
 - 3 Calculate $S(r^*)$ by Eq. (1) using either observed data $(r_i)_{i=1}^n$ or synthetic data from the learned generative model
 - 4 Calculate noises in the target sample by Eq. (3)
 - 5 **for** each p in $1, \dots, d+2$ **do**
 - 6 Initialize $\phi(p) \leftarrow 0$
 - 7 **for** each set $I \in 2^{\{1, \dots, d+2\} \setminus \{p\}}$ **do**
 - 8 calculate $\phi(p|I)$ using Eq. (4) by generating synthetic data
 - 9 $\phi(p) \leftarrow \phi(p) + (d+2)^{-1} \binom{d+1}{|I|}^{-1} \phi(p|I)$
 - 10 **end**
 - 11 **end**
-

2.3. The case of time-series data

Suppose that, instead of n i.i.d. samples, we are given time-series data $D_{\text{train}} = (X_{t,1}, \dots, X_{t,d}, Y_t, r_t)_{t=1}^T$ and a target outlier sample $((x_{t^*,p}^*)_{p=1}^d, y_{t^*}, r_{t^*})$ at some time-step t^* . We want to calculate the outlier score $S(r_{t^*})$ and the attributions $\phi(p)$ to this score. Algorithm 1 can be adapted to this case.

For time-series data, we assume the following stationary discrete-time autoregressive process with additive noises:

$$X_{t,p} = g_p((X_{t,q})_{q \in \text{pa}(t,p)}) + N_{t,p}, \quad p = 1, \dots, d+2, \quad (7)$$

where $pa(t, p) = \{X_{t', q} \mid t' \leq t\}$ is the set of parents of $X_{t, p}$, and $N_{t, p}$ is the noise at the variable $X_{t, p}$. Comparing with the general time-series functional causal model in [Runge et al. \(2019\)](#), this model is a special case where the noise at each variable is additive.

The time-series data from this model can be approximately converted to a non-time series data as follows. Define τ_{max} as the order of the time-series. This means that, a variable $X_{t, p}$ is not a parent of any variable $X_{t+\tau, q}$ with $\tau > \tau_{max}$. This implies that $X_{t, p}$ and $X_{t+\tau_{max}+1, p}$ can be approximately treated as independent samples from a same variable X_p . Therefore, we can create a new non-time-series dataset of $(d + 2) \times (\tau_{max} + 1)$ variables: X_1 at lag 0, \dots , X_{d+2} at lag 0, X_1 at lag 1, \dots , X_{d+2} at lag 1, \dots , X_1 at lag τ_{max} , \dots , X_{d+2} at lag τ_{max} to approximate the original time-series. The framework in [Algorithm 1](#) can then be applied to this dataset.

With this converted time-lagged dataset, [Algorithm 1](#) will output the attribution of a variable X_p at multiple time lags: $\phi(X_p \text{ at lag } 0)$, $\phi(X_p \text{ at lag } 1)$, \dots , $\phi(X_p \text{ at lag } \tau_{max})$. We will use their sum as the final attribution of X_p :

$$\phi(p) = \sum_{\tau=0}^{\tau_{max}} \phi(X_p \text{ at lag } \tau). \quad (8)$$

2.4. Discussion

2.4.1. THE CHOICE OF THE CAUSAL DISCOVERY ALGORITHM

For non-time-series data, one can use constraint-based algorithms such as the Peter-Clark (PC) algorithm ([Spirtes et al., 2001](#)), or methods based on functional causal models such as the DirectLiNGAM algorithm ([Shimizu et al., 2011](#)) to estimate the causal graph.

For time-series data, there are two ways to estimate the causal graph. The first way is to use time-series specific algorithms on the original time-series data. Some examples are constraint-based time-series algorithm PCMCI ([Runge et al., 2019](#)) and its bootstrap aggregation extension ([Debeire et al., 2024](#)), and the time-series algorithm VARLiNGAM that is based on functional causal models ([Hyvärinen et al., 2010](#)). Alternatively, one can apply the PC or DirectLiNGAM algorithm on the converted lagged data.

2.4.2. THE CHOICE OF REGRESSION MODELS AND PARAMETRIC NOISE DISTRIBUTIONS

We use the `dowhy-gcm` package ([Blöbaum et al., 2024](#)) to learn the regression model for g_p and parametric distribution for the noise N_p . This implementation includes a wide range of regression methods as well as rich families of parametric distributions, and cross-validation methods for selecting the optimal ones. We use the default options of the package in our experiments.

3. Numerical results

In this section, we will compare our method with existing approaches in detecting root causes for prediction errors in both time-series and non-time-series data. We also investigate the limitations and sensitivity of our proposed approach.

For baselines used in comparisons, the following methods, whose implementations are adapted from Python scripts of [Idé and Abe \(2023\)](#), are used.

z-score Given a target sample $((x_p^*)_{p=1}^d, y^*, r^*)$ where we want to measure the attribution of each variable X_p ($p = 1, \dots, d + 1$) to the outlierness of the prediction error r^* , we use z-score for the attribution: $\phi^z(p) = (x_p^* - \mu_p)/\sigma_p$, where μ_p and σ_p are the mean and standard deviation of X_p in D_{train} , respectively. The intuition behind the z-score approach is that the outlierness of r^* is caused directly by the outlierness of x_p^* .

LIME As another baseline method, we use LIME proposed by Ribeiro et al. (2016). For a target sample $((x_p^*)_{p=1}^d, y^*, r^*)$, denote the covariate vector $[x_1^*, \dots, x_d^*]^\top$ as \mathbf{x}^* . The attribution of X_p ($p = 1, \dots, p$), denoted as $\phi^{LIME}(p)$, is defined as the coefficient β_p of the following length- d coefficient vector β^* :

$$\beta^* = \operatorname{argmin}_{\beta \in \mathbb{R}^d} \frac{1}{N_s} \sum_{n=1}^{N_s} \left(f(\mathbf{x}^{[n]}) - y^* - \beta^\top \mathbf{x}^{[n]} \right)^2 + \lambda \|\beta\|, \quad (9)$$

where $f(\mathbf{x})$ is the prediction value of the prediction model at \mathbf{x} , and $\mathbf{x}^{[n]} = [x_1^{[n]}, \dots, x_d^{[n]}]^\top$ ($n = 1, \dots, N_s$) is a length- d random vector sampled from the multivariate normal distribution $\mathcal{N}(\mathbf{x}^*, \sigma_x \mathbf{I}_{d \times d})$ (σ_x set at 0.01). Intuitively, LIME measures the influence of each covariate in explaining the prediction error $f(\mathbf{x}^{[n]}) - y^*$ by using the linear model $\beta^\top \mathbf{x}^{[n]}$ as a surrogate model.

In Section 3.1, we provide an example to showcase the working of our method CD-RCA, comparing with these two existing approaches. We then provide various sensitivity analyses of CD-RCA in Sections 3.2, 3.3, and 3.4.

3.1. An illustrative example

We consider synthetic time-series data generated from the model in Eq. (7). In this example, there are three covariates X_1, X_2, X_3 , and a target variable $Y = X_4$. The causal relationships between them are described in Fig. 1A. Twenty thousand samples of $((X_p)_{p=1}^3, Y)$ were generated from the causal model described in Eq. (B.1).

Using the first 10000 sample, we trained a time-series prediction model proposed in Runge et al. (2015). This trained model would be subsequently used as the black-box prediction model f . We then augmented each sample of $((X_p)_{p=1}^3, Y)$ in the last 10000 samples with the corresponding prediction error r from the prediction model. The final samples are of the form $((X_p)_{p=1}^3, Y, r)$, and constitute our training data D_{train} for Algorithm 1.

To generate a target outlier sample, we first generated a new time-series of $((X_p)_{p=1}^3, Y)$ from Eq. (B.1). When generating the sample at the 500-th time-step, we first generated a clean X_1 based on Eq. (B.1), then added an outlier noise $Z = 20$ to the result. We then used the contaminated value of X_1 , together with X_3 , to generate X_2 , and then Y , based on Eq. (B.1). This contaminated sample is then put into the prediction model f to obtain the prediction error r . Since the value of X_1 was unusually large, the value of r was unusually large, too, i.e., X_1 is the root cause for the outlier value of r . The augmented sample of $((X_p)_{p=1}^3, Y, r)$ is then chosen as the target outlier sample.

For estimating the causal graph from D_{train} in CD-RCA, we use the PCMCI algorithm with bootstrap aggregation (Debeire et al., 2024) with number of bootstrap samples set at 500 as the causal discovery algorithm in Algorithm 1. For each run of Algorithm 1, we obtained one set of attribution values. Due to randomness in line 8 of the algorithm, we repeated Algorithm 1 50 times to obtain 50 sets of attribution values.

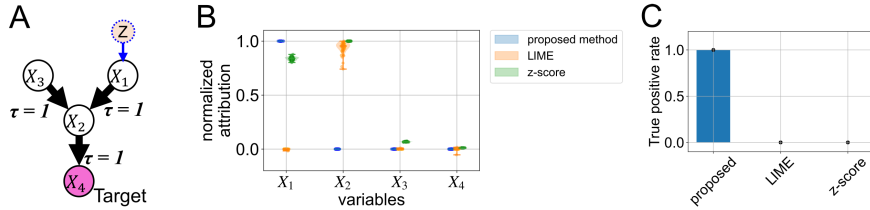


Figure 1: **Root cause detection for prediction error outlier in time-series data.** (A) The true causal graph. The prediction target variable is $Y = X_4$. The root-cause for the outlier sample is X_1 . (B) Normalized attribution of each variable provided by each method. The probability densities in the violin plots were calculated using a kernel density method based on attribution values from 50 trials. The error bar indicates the maximum and minimum values of the attributions. (C) True positive rate in identifying X_1 as the root cause of each method.

We also matched this number for z-score and LIME. For z-score, we sampled randomly with replacement from D_{train} 50 subsets, each contains 5000 samples, and calculated the z-score attributions in each subset to obtain 50 sets of attribution values. For LIME, we changed the random seed 50 times when generating synthetic data from the multivariate normal distribution.

Figure 1B shows the normalized attribution of each variable over 50 sets of attribution values. Both z-score and LIME method wrongly gave the largest attribution to X_2 , while CD-RCA successfully gave X_1 the highest attribution. Fig. 1C shows the true positive rate in successfully identifying X_1 as the root cause. Both z-score and LIME could not identify X_1 as their true positive rates are both 0, while CD-RCA successfully identified X_1 as the root-cause of the outlier.

To *predict* the value of Y , the value of X_2 alone is enough, while in the absence of X_2 both value of X_1 and X_3 are needed. In a sense, this implies that X_2 might be the most important variable in predicting Y . This is the reason LIME picked out X_2 as the root cause, and this example shows that focusing only on powers in predicting Y is not enough. Since CD-RCA considers the causal relationships between all variables, it could successfully detect the root cause as X_1 .

3.2. Effects of outlier magnitude and average total effect on CD-RCA

Since the attribution $\phi(p)$ in CD-RCA is based on the Shapley value proposed by Budhathoki et al. (2022), the reliability of CD-RCA would be directly affected by the RCA performance of this particular version of the Shapley value. In this experiment, we evaluated the sensitivity of only the RCA part to changes in amplitudes of anomalous noises and changes in causal mechanisms. To isolate the RCA performance from other parts of CD-RCA, although we still execute line 2 of Algorithm 1 to learn the generative model from the observed data, we do not estimate the causal graph, i.e., line 1 in Algorithm 1, and use the true causal graph. Furthermore, we do not include prediction errors, and choose another variable where we will pick out an outlier sample and measure its outlier score. Nevertheless, we expect the sensitivity result of this experiment would also apply to the full version of CD-RCA, a point we indeed confirmed in Section 3.4.

The causal mechanisms for training data were based on the two models F_1 and F_2 in Eqs. (B.2) and (B.3), respectively. These models constructed with three covariates X_p ($p = 1, \dots, 3$) and a target variable X_4 , where we will measure its outlier score and the attributions of the remaining variables to the score (see Appendix B.2.1).

For the target outlier sample, we will use different causal models compared to the training data. Specifically, the outlier samples corresponding to training data generated from F_1 and F_2 were generated from three models in Eqs. (B.4)–(B.6) and three models in Eqs. (B.7)–(B.9), respectively. These models for outlier samples have the same causal graphs as in F_1 and F_2 , but with tunable coefficients β of some edge and different locations of where we will add the anomalous noise Z . The amplitude of Z can also be controlled. The root-cause Z was added to one of the observational variables X only at the 500-th sample, and this sample is chosen to be the target outlier sample. See Appendix B.2.1 for more details.

By using the generated target outlier samples with the above procedures, the attribution ϕ in the target sample were evaluated by using CD-RCA with known causal graphs F_1 and F_2 . Moreover, for quantifying the root cause detection accuracy, the values of ϕ were repetitively estimated 50 times for all parameter conditions of β and Z for each model. After these estimations were finished, the RCA accuracy for each model was calculated for all parameter conditions. A successful detection was defined as when the variable with the maximum value of the attribution $\phi(p)$ is the same as where we added Z in the outlier sample.

The results with model F_1 are shown in Fig. 2A–C. Fig. 2A, B indicated that the RCA accuracy tends to be high regardless of the value of edge coefficient β under the condition $Z \gg 0.5$. Since the exogenous noise N_p at each X_p follows the uniform distribution $\mathcal{U}(0, 1)$ with mean 0.5, these results suggested that the detection is successful when $Z \geq \mathbb{E}[N_p]$. However, the result in Fig. 2C showed a different tendency: the accuracy tends to be lower when $Z \leq \beta$. One explanation is that the effect of Z on X_2 becomes relatively lower than that of X_1 on X_2 when $Z \leq \beta$, and thus X_1 tends to be wrongly identified as the root-cause in Fig. 2C.

In contrast to the results with F_1 in Fig. 2A–C, the results with F_2 in Fig. 2D–F showed a different tendency. Even though the causal graph in F_2 is the same as in F_1 , some edge coefficients in the causal graph were set to a smaller value relative to those in F_1 (see Eqs. (B.2) and (B.3)). These differences were reflected in the differences in the average total effects (ATE) to the target variable X_4 . Since the $ATE_{X_1 \rightarrow X_4}$ in F_2 , as can be seen from Fig. 3B, were almost zero, i.e., X_1 has no causal effect on X_4 , the high accuracy of RCA are not found unless the amplitude of Z is large enough in Fig. 2D. The same phenomenon happened in Fig. 2F. Since the $ATE_{X_2 \rightarrow X_4}$ in F_2 , as can be seen in Fig. 3B, were relatively higher than zero, the RCA performance in Fig. 2E showed similar tendency as that of Fig. 2B.

Considering the above results, the CD-RCA method might encounter difficulties in detecting the root cause variable when: (1) the amplitude of Z is smaller than the observational noise N , or (2) the root cause variable has no causal effect on the target variables. We also conducted a similar sensitivity analysis in non-time-series case (Appendix B.2.2), and found the same tendency (Fig. B.1).

3.3. Effects of sample sizes on CD-RCA

In this simulation, we aimed to reveal how the root cause detection accuracy in CD-RCA is affected by the sample size of the training data. We applied the CD-RCA to the synthetic time-series data without any prior knowledge of causal structures.

The causal graph was estimated from training dataset with PCMCI with bootstrap aggregation algorithm (Debeire et al., 2024). 20000 samples based on the Eq. (B.18) were generated. This synthetic data consisted with three covariates X_p ($p = 1, \dots, 3$) and a target variable $Y =$

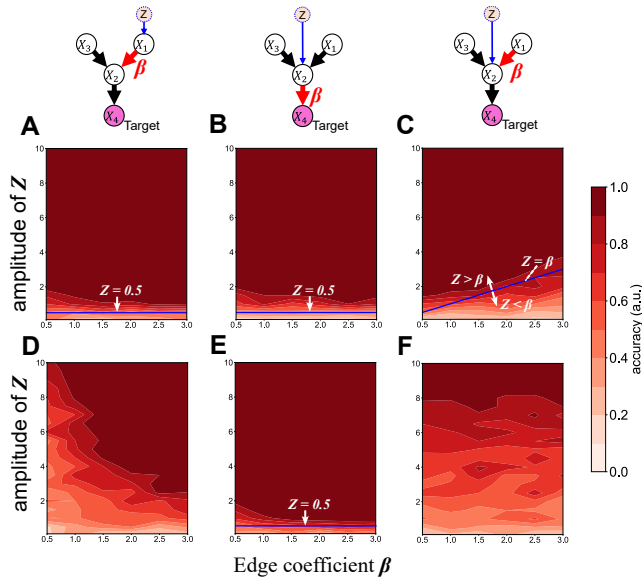


Figure 2: **Effects of outlier magnitude and average total effect to target variable on the performance of CD-RCA.** (A–C) The results of the root cause detection accuracy, relative to the changes in amplitude of Z and graph edge weight β in the model F_1 . The causal graph diagram of each panel indicates the location of the exact root-cause (Z) and edge changes (β) for each simulation settings. (D–F) The results of the model F_2 in the same manner of (A–C).

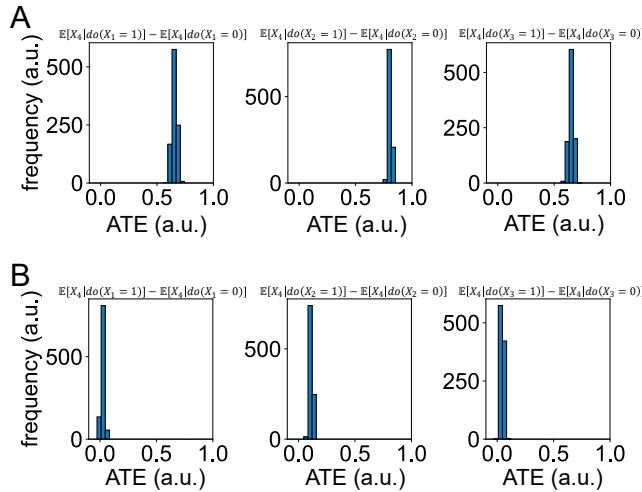


Figure 3: **Total effect to target variable X_4 in the models for training data.** A) Average total effect: ATE in the model F_1 , from X_1 to X_4 , from X_2 to X_4 , and from X_3 to X_4 , respectively. B) ATE results of F_2 in the same manner in F_1 . These results were obtained from causal models F_1 and F_2 by the `dowhy-gcm` package.

X_4 . In this simulation, we use the PCMCI with bootstrap aggregations (Debeire et al., 2024) for estimating the causal graph in Algorithm 1 with different sample size conditions ($N_{sample} = [500, 1000, 5000, 10000, 20000]$). The bootstrap sample number was set as 500. As the same reason in the Section 3.1, the graph estimation in Algorithm 1 was repeated 10 times (i.e., 10 causal graphs were estimated for each sample size).

After learning the causal graph \mathcal{G} for each sample size, we tested the root cause detection accuracy in the target outlier sample. The target outlier samples were generated by the model F_{sim2}^{test} that consisted with the same causal structures in F_{sim2}^{train} ; however, the anomalous noise Z was added to the variable X_1 only at the 500-th time-step (see the Eq. (B.19)). The sample at this time-step is then chosen as the target outlier sample.

The attributions $\phi(p)$ were calculated at the target outlier sample for all 10 causal graphs. Therefore, we can obtain 10 samples of $\phi(p)$ for each p in each sample size. See Appendix B.3.1 for more details of this simulation.

The results are shown in Fig. 4. We found that the estimated attribution in X_1 is the largest regardless the sample size. As can be seen in the model settings in Eq. (B.18), the edge coefficients $\beta_{X_1 \rightarrow X_2}$ and $\beta_{X_2 \rightarrow X_4}$, corresponding to the causal pathway from X_1 (i.e., the root cause variable) to X_4 (the target variable), are large. One might be tempted to think that such settings would make a strong bias for X_2 mediating the causal pathway from X_1 to X_4 , leading to false detections of the root cause. Fig. 4 showed that such intuition is false: the highest causal attribution is detected in X_1 regardless of the sample size, indicating that CD-RCA can correctly detect the root cause in such cases.

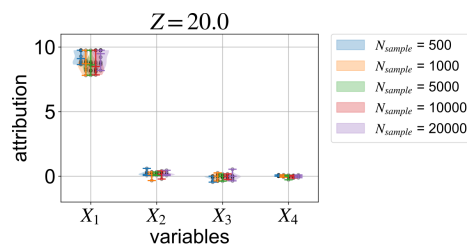


Figure 4: **Effect of the sample size in the time-series causal discovery for CD-RCA.** The probability densities in these violin plots were calculated using a kernel density method based on the samples of the attribution values. The error bar indicates the maximum and minimum values of samples.

3.4. Comparisons with baseline methods in non-time-series data

In this experiment, we compared the root-cause detecting performance of CD-RCA with baselines in non-time-series data, under different amplitudes of the outlier noise Z . Changing the noise amplitude also allows us to check the failure condition of CD-RCA observed in Section 3.2.

Twenty thousand samples of $((X_p)_{p=1}^3, X_4)$ were generated from the model in Eq. (B.20). A L1 sparse regressions model f was trained on the first 10000 samples to predict $Y = X_4$ with $(X_p)_{p=1}^3$ as covariates, by the `LassoCV` module in the `scikit-learn` Python package. The learned f is then used to calculate the corresponding prediction errors r of in the last 10000 samples. The augmented samples of the form $((X_p)_{p=1}^3, Y, r)$ from the last 10000 samples constitute the training data D_{train} for Algorithm 1.

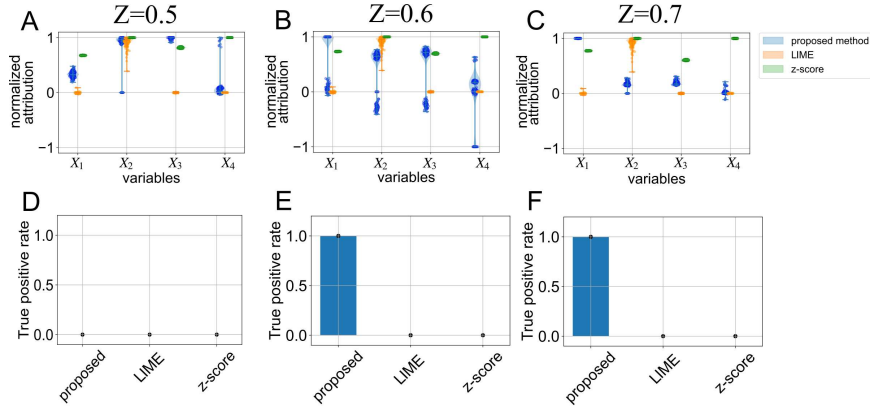


Figure 5: **Comparisons of RCA performance in non-time-series data.** (A–C) Comparisons of the RCA performance in our method with baseline method for each value of Z (A: $Z = 0.5$, B: $Z = 0.6$, C: $Z = 0.7$). The probability densities in these violin plots show the results in same manner in Fig. 4. (D–F) True positive rate of each method in (A–C).

The target outlier sample was generated from the model F_{sim3}^{test} in Eq. (B.21) in the same way as in previous simulations. The root-cause Z was applied to X_1 only at 500-th sample in the synthetic data generated by F_{sim3}^{test} . We considered three values for the amplitude of Z : 0.5, 0.6, and 0.7.

We use DirectLiNGAM with bootstrapping (Shimizu et al., 2011; Thamvitayakul et al., 2012) as the causal discovery algorithm in Algorithm 1. The bootstrap sample number was set at 500. For each p , the attribution $\phi(p)$ was evaluated for all 500 bootstrap causal graphs.

To match the number of attribution samples, for 500 times, we randomly sample 5000 samples from D_{train} and calculate the $\phi^z(p)$ in the subset. For LIME, we changed the random seed when calculating $\phi^{LIME}(p)$ 500 times to get 500 values of $\phi^{LIME}(p)$ for each p .

Figure 5 showed the results. As shown in Fig. 5 A–C, our method correctly determined the largest attribution value at X_1 when $Z > 0.5 = \mathbb{E}[N_{back}]$, the average background observation noise. The false detection of our method when $Z \leq 0.5$ (Fig. 5A) is consistent with the limitation of the CD-RCA method discussed in Section 3.2, indicating that CD-RCA cannot correctly detect the root cause when $Z \leq \mathbb{E}[N_{back}]$.

On the other hand, both baseline methods cannot detect the location of the root cause regardless of the value of Z . Particularly, LIME falsely produced the largest attribution at X_2 for all values of Z , the same result as in Fig 1. These contrastive results between our method and baseline methods would emphasize that considering the causal mechanism of the prediction error is crucial for RCA.

4. Conclusions

In this study, we tested our proposed CD-RCA method for detecting the root cause variable for outliers in prediction errors of black-box ML systems. By numerical simulations, we confirmed the advantages of our method relative to existing heuristic attribution methods. Moreover, we discovered that the Shapley value might encounter difficulties in detecting the root cause variable when: (1) the amplitude of the root cause Z is lower than that of the observational noise, or (2) there is no causal effect from the root cause variable to the target variable.

In addition to the above-mentioned limitation, another issue with the method is that it assumes causal sufficiency in the observational data, meaning no other confounding factors involving the unobserved root cause Z . Therefore, future work should consider the effect of unobserved confounding factors for our proposed method. As a possible solution to address this issue, we can use the LPCMCI algorithm (Gerhardus and Runge (2020); PCMCI with latent confounding factors) instead of PCMCI. By using LPCMCI to estimate the causal mechanisms of the prediction error, our proposed method can be used to apply the RCA task under the causal insufficient system. In addition, by combining the LPCMCI with the method for estimating the causal effect boundary (Malinsky and Spirtes, 2017) in causal insufficient systems, we would sufficiently detect the possible causal structures while considering the distinctiveness issue of the Markov equivalence class under the possibly confounded systems.

Despite such a limitation, our method provides advantages over the conventional algorithms in the RCA task for understanding the generative mechanisms of the prediction error in ML models.

Acknowledgments

The research was the collaborative work of Toshiba Corporation and Shiga University, based on funding from Toshiba Corporation.

References

- Patrick Blöbaum, Peter Götz, Kailash Budhathoki, Atalanti A. Mastakouri, and Dominik Janzing. DoWhy-GCM: An extension of DoWhy for causal inference in graphical causal models. *Journal of Machine Learning Research*, 25(147):1–7, 2024. URL <http://jmlr.org/papers/v25/22-1258.html>.
- Kailash Budhathoki, Lenon Minorics, Patrick Blöbaum, and Dominik Janzing. Causal structure-based root cause analysis of outliers. In Kamalika Chaudhuri, Stefanie Jegelka, Le Song, Csaba Szepesvari, Gang Niu, and Sivan Sabato, editors, *Proceedings of the 39th International Conference on Machine Learning*, volume 162 of *Proceedings of Machine Learning Research*, pages 2357–2369. PMLR, 17–23 Jul 2022. URL <https://proceedings.mlr.press/v162/budhathoki22a.html>.
- Vanessa Buhmester, David Münch, and Michael Arens. Analysis of explainers of black box deep neural networks for computer vision: A survey. *Machine Learning and Knowledge Extraction*, 3(4):966–989, 2021. ISSN 2504-4990. doi: 10.3390/make3040048. URL <https://www.mdpi.com/2504-4990/3/4/48>.
- Vinay Chamola, Vikas Hassija, A Razia Sulthana, Debshishu Ghosh, Divyansh Dhingra, and Biplab Sikdar. A review of trustworthy and explainable artificial intelligence (XAI). *IEEE Access*, 11: 78994–79015, 2023. doi: 10.1109/ACCESS.2023.3294569.
- Kevin Debeire, Andreas Gerhardus, Jakob Runge, and Veronika Eyring. Bootstrap aggregation and confidence measures to improve time series causal discovery. In Francesco Locatello and Vanessa Didelez, editors, *Proceedings of the Third Conference on Causal Learning and Reasoning*, volume 236 of *Proceedings of Machine Learning Research*, pages 979–1007. PMLR, 01–03 Apr 2024. URL <https://proceedings.mlr.press/v236/debeire24a.html>.

Huiqi Deng, Na Zou, Mengnan Du, Weifu Chen, Guocan Feng, and Xia Hu. A unified Taylor framework for revisiting attribution methods. In *Thirty-Fifth AAAI Conference on Artificial Intelligence, AAAI 2021, Thirty-Third Conference on Innovative Applications of Artificial Intelligence, IAAI 2021, The Eleventh Symposium on Educational Advances in Artificial Intelligence, EAAI 2021, Virtual Event, February 2-9, 2021*, pages 11462–11469. AAAI Press, 2021. doi: 10.1609/AAAI.V35I13.17365. URL <https://doi.org/10.1609/aaai.v35i13.17365>.

Huiqi Deng, Na Zou, Mengnan Du, Weifu Chen, Guocan Feng, Ziwei Yang, Zheyang Li, and Quanshi Zhang. Unifying fourteen post-hoc attribution methods with Taylor interactions. *IEEE Trans. Pattern Anal. Mach. Intell.*, 46(7):4625–4640, January 2024. ISSN 0162-8828. doi: 10.1109/TPAMI.2024.3358410. URL <https://doi.org/10.1109/TPAMI.2024.3358410>.

Andreas Gerhardus and Jakob Runge. High-recall causal discovery for autocorrelated time series with latent confounders. In H. Larochelle, M. Ranzato, R. Hadsell, M.F. Balcan, and H. Lin, editors, *Advances in Neural Information Processing Systems*, volume 33, pages 12615–12625. Curran Associates, Inc., 2020. URL https://proceedings.neurips.cc/paper_files/paper/2020/file/94e70705efae423efda

Michel Grabisch and Marc Roubens. An axiomatic approach to the concept of interaction among players in cooperative games. *Game Theory*, 28:547–565, 1999. doi: 10.1007/s001820050125.

Riccardo Guidotti, Anna Monreale, Salvatore Ruggieri, Franco Turini, Fosca Giannotti, and Dino Pedreschi. A survey of methods for explaining black box models. *ACM Comput. Surv.*, 51(5), August 2018. ISSN 0360-0300. doi: 10.1145/3236009. URL <https://doi.org/10.1145/3236009>.

Joseph Y. Halpern and Christopher Hitchcock. Graded causation and defaults. *British Journal for the Philosophy of Science*, 66(2):413–457, 2015. doi: 10.1093/bjps/axt050.

Vikas Hassija, Vinay Chamola, Atmesh Mahapatra, Abhinandan Singal, Divyansh Goel, Kaizhu Huang, Simone Scardapane, Indro Spinelli, Mufti Mahmud, and Amir Hussain. Interpreting black-box models: A review on explainable artificial intelligence. *Cognitive Computation*, 16: 45–74, 2023. URL <https://api.semanticscholar.org/CorpusID:261154217>.

Tom Heskes, Ioan Gabriel Bucur, Evi Sijben, and Tom Claassen. Causal Shapley values: Exploiting causal knowledge to explain individual predictions of complex models. In *Proceedings of the 34th International Conference on Neural Information Processing Systems, NIPS '20*, Red Hook, NY, USA, 2020. Curran Associates Inc. ISBN 9781713829546.

Patrik Hoyer, Dominik Janzing, Joris M Mooij, Jonas Peters, and Bernhard Schölkopf. Nonlinear causal discovery with additive noise models. In D. Koller, D. Schuurmans, Y. Bengio, and L. Bottou, editors, *Advances in Neural Information Processing Systems*, volume 21. Curran Associates, Inc., 2008. URL https://proceedings.neurips.cc/paper_files/paper/2008/file/f7664060cc52bc6f3d6

Xuanxiang Huang and Joao Marques-Silva. On the failings of Shapley values for explainability. *Int. J. Approx. Reasoning*, 171(C), August 2024. ISSN 0888-613X. doi: 10.1016/j.ijar.2023.109112. URL <https://doi.org/10.1016/j.ijar.2023.109112>.

- Aapo Hyvärinen, Kun Zhang, Shohei Shimizu, and Patrik O. Hoyer. Estimation of a structural vector autoregression model using non-gaussianity. *Journal of Machine Learning Research*, 11(56):1709–1731, 2010. URL <http://jmlr.org/papers/v11/hyvarinen10a.html>.
- Tsuyoshi Idé and Naoki Abe. Generative perturbation analysis for probabilistic black-box anomaly attribution. In *Proceedings of the ACM SIGKDD International Conference on Knowledge Discovery and Data Mining*, pages 845–856. Association for Computing Machinery, 8 2023. ISBN 9798400701030. doi: 10.1145/3580305.3599365.
- Tsuyoshi Idé, Amit Dhurandhar, Jiří Navrátil, Moninder Singh, and Naoki Abe. Anomaly attribution with likelihood compensation. *Proceedings of the AAAI Conference on Artificial Intelligence*, 35(5):4131–4138, May 2021. doi: 10.1609/aaai.v35i5.16535. URL <https://ojs.aaai.org/index.php/AAAI/article/view/16535>.
- Dominik Janzing, Patrick Blöbaum, Atalanti A Mastakouri, Philipp M Faller, Lenon Minorics, and Kailash Budhathoki. Quantifying intrinsic causal contributions via structure preserving interventions. In Sanjoy Dasgupta, Stephan Mandt, and Yingzhen Li, editors, *Proceedings of The 27th International Conference on Artificial Intelligence and Statistics*, volume 238 of *Proceedings of Machine Learning Research*, pages 2188–2196. PMLR, 02–04 May 2024. URL <https://proceedings.mlr.press/v238/janzing24a.html>.
- Yonghan Jung, Shiva Kasiviswanathan, Jin Tian, Dominik Janzing, Patrick Bloebaum, and Elias Bareinboim. On measuring causal contributions via do-interventions. In Kamalika Chaudhuri, Stefanie Jegelka, Le Song, Csaba Szepesvari, Gang Niu, and Sivan Sabato, editors, *Proceedings of the 39th International Conference on Machine Learning*, volume 162 of *Proceedings of Machine Learning Research*, pages 10476–10501. PMLR, 17–23 Jul 2022. URL <https://proceedings.mlr.press/v162/jung22a.html>.
- Davinder Kaur, Suleyman Uslu, Kaley J. Rittichier, and Arjan Durrresi. Trustworthy artificial intelligence: A review. *ACM Comput. Surv.*, 55(2), January 2022. ISSN 0360-0300. doi: 10.1145/3491209. URL <https://doi.org/10.1145/3491209>.
- Bo Li, Peng Qi, Bo Liu, Shuai Di, Jingen Liu, Jiquan Pei, Jinfeng Yi, and Bowen Zhou. Trustworthy AI: From principles to practices. *ACM Comput. Surv.*, 55(9), January 2023. ISSN 0360-0300. doi: 10.1145/3555803. URL <https://doi.org/10.1145/3555803>.
- Sisi Ma and Roshan Tourani. Predictive and causal implications of using Shapley value for model interpretation. In *Proceedings of the 2020 KDD Workshop on Causal Discovery*, volume 127 of *Proceedings of Machine Learning Research*, pages 23–38. PMLR, 24 Aug 2020. URL <https://proceedings.mlr.press/v127/ma20a.html>.
- Osama Makansi, Julius Von Kügelgen, Francesco Locatello, Peter Vincent Gehler, Dominik Janzing, Thomas Brox, and Bernhard Schölkopf. You mostly walk alone: Analyzing feature attribution in trajectory prediction. In *International Conference on Learning Representations*, 2022. URL <https://openreview.net/forum?id=POxF-LEqnF>.
- Daniel Malinsky and Peter Spirtes. Estimating bounds on causal effects in high-dimensional and possibly confounded systems. *International Journal of Approximate Reasoning*, 88:371–384, 9 2017. ISSN 0888613X. doi: 10.1016/j.ijar.2017.06.005.

- Atalanti A Mastakouri, Bernhard Schölkopf, and Dominik Janzing. Necessary and sufficient conditions for causal feature selection in time series with latent common causes. In Marina Meila and Tong Zhang, editors, *Proceedings of the 38th International Conference on Machine Learning*, volume 139 of *Proceedings of Machine Learning Research*, pages 7502–7511. PMLR, 18–24 Jul 2021. URL <https://proceedings.mlr.press/v139/mastakouri21a.html>.
- Marco Tulio Ribeiro, Sameer Singh, and Carlos Guestrin. "Why Should I Trust You?": Explaining the predictions of any classifier. In *Proceedings of the 22nd ACM SIGKDD International Conference on Knowledge Discovery and Data Mining*, KDD '16, page 1135–1144, New York, NY, USA, 2016. Association for Computing Machinery. ISBN 9781450342322. doi: 10.1145/2939672.2939778. URL <https://doi.org/10.1145/2939672.2939778>.
- Jakob Runge, Reik V. Donner, and Jürgen Kurths. Optimal model-free prediction from multivariate time series. *Physical Review E - Statistical, Nonlinear, and Soft Matter Physics*, 91, 5 2015. ISSN 15502376. doi: 10.1103/PhysRevE.91.052909.
- Jakob Runge, Peer Nowack, Marlene Kretschmer, Seth Flaxman, and Dino Sejdinovic. Detecting and quantifying causal associations in large nonlinear time series datasets. *Science Advances*, 5(11):eaau4996, 2019. doi: 10.1126/sciadv.aau4996. URL <https://www.science.org/doi/abs/10.1126/sciadv.aau4996>.
- L. S. Shapley. 17. A value for n-person games. In Harold William Kuhn and Albert William Tucker, editors, *Contributions to the Theory of Games, Volume II*, pages 307–318. Princeton University Press, Princeton, 1953. ISBN 9781400881970. doi: doi:10.1515/9781400881970-018. URL <https://doi.org/10.1515/9781400881970-018>.
- Shohei Shimizu, Takanori Inazumi, Yasuhiro Sogawa, Aapo Hyvärinen, Yoshinobu Kawahara, Takashi Washio, Patrik O. Hoyer, and Kenneth Bollen. DirectLiNGAM: A direct method for learning a linear non-gaussian structural equation model. *J. Mach. Learn. Res.*, 12(null): 1225–1248, July 2011. ISSN 1532-4435.
- Peter Spirtes, Clark Glymour, and Richard Scheines. *Causation, Prediction, and Search*. The MIT Press, 01 2001. ISBN 9780262284158. doi: 10.7551/mitpress/1754.001.0001. URL <https://doi.org/10.7551/mitpress/1754.001.0001>.
- Kittitat Thamvitayakul, Shohei Shimizu, Tsuyoshi Ueno, Takashi Washio, and Tatsuya Tashiro. Bootstrap confidence intervals in DirectLiNGAM. In *2012 IEEE 12th International Conference on Data Mining Workshops*, pages 659–668, 2012. doi: 10.1109/ICDMW.2012.134.
- Jianlong Zhou, Amir H. Gandomi, Fang Chen, and Andreas Holzinger. Evaluating the quality of machine learning explanations: A survey on methods and metrics. *Electronics*, 10(5), 2021. ISSN 2079-9292. doi: 10.3390/electronics10050593. URL <https://www.mdpi.com/2079-9292/10/5/593>.

Appendix A. Related works

Given its practical importance, there is a vast literature on attribution methods. Some recent attribution methods that do not incorporate causality are [Deng et al. \(2021\)](#), [Deng et al. \(2024\)](#), [Idé et al. \(2021\)](#), and [Idé and Abe \(2023\)](#). Some attribution methods that utilize causality are [Heskes et al. \(2020\)](#), [Jung et al. \(2022\)](#), and [Janzing et al. \(2024\)](#). An application of Shapley-value-based attribution methods is provided in [Makansi et al. \(2022\)](#). A related work on feature selection in time-series is [Mastakouri et al. \(2021\)](#).

Appendix B. Additional materials for experiments

B.1. Illustrative example

We use the following linear causal model:

$$F^{train} = \begin{cases} X_1^t = 0.8X_1^{t-1} + N_{X_1} \\ X_2^t = 3.8X_1^{t-1} + 0.8X_3^{t-1} + N_{X_2} \\ X_3^t = 0.8X_3^{t-1} + N_{X_3} \\ X_4^t = 3.8X_2^{t-1} + N_{X_4} \end{cases} \quad (\text{B.1})$$

where $N_{X_n} \sim \mathcal{U}(0, 1)$.

B.2. Effects of outlier magnitude and average total effect

B.2.1. MODEL SETTINGS

In this section, we explained the details in the equations for generating the synthetic time-series data in the Section 3.2. As mentioned in this section, we applied two different models F_1 and F_2 for the exact causal mechanisms in this simulation. The models F_1 and F_2 are based on the following equations. These models are applied as the causal mechanisms for evaluating the causal attributions of each observed variables for the target anomalous sample.

$$F_1 := \begin{cases} X_1^t = 0.8X_1^{t-1} + N_{X_1} \\ X_2^t = 0.8X_1^{t-1} + 0.8X_3^{t-1} + N_{X_2} \\ X_3^t = 0.8X_3^{t-1} + N_{X_3} \\ X_4^t = 0.8X_2^{t-1} + N_{X_4} \end{cases} \quad (\text{B.2})$$

$$F_2 := \begin{cases} X_1^t = 0.2X_1^{t-1} + N_{X_1} \\ X_2^t = 0.2X_1^{t-1} + 0.4X_3^{t-1} + N_{X_2} \\ X_3^t = 0.2X_3^{t-1} + N_{X_3} \\ X_4^t = 0.1X_2^{t-1} + N_{X_4} \end{cases} \quad (\text{B.3})$$

The target anomalous sample for the model F_1 was generated by the following models:

$$F_{1_{testA}} := \begin{cases} X_1^t = 0.8X_1^{t-1} + N_{X_1} + Z \\ X_2^t = \beta X_1^{t-1} + 0.8X_3^{t-1} + N_{X_2} \\ X_3^t = 0.8X_3^{t-1} + N_{X_3} \\ X_4^t = 0.8X_2^{t-1} + N_{X_4} \end{cases} \quad (\text{B.4})$$

$$F_{1_{testB}} := \begin{cases} X_1^t = 0.8X_1^{t-1} + N_{X_1} \\ X_2^t = 0.8X_1^{t-1} + 0.8X_3^{t-1} + N_{X_2} + Z \\ X_3^t = 0.8X_3^{t-1} + N_{X_3} \\ X_4^t = \beta X_2 + N_{X_4} \end{cases} \quad (\text{B.5})$$

$$F_{1_{testC}} := \begin{cases} X_1^t = 0.8X_1^{t-1} + N_{X_1} \\ X_2^t = \beta X_1^{t-1} + 0.8X_3^{t-1} + N_{X_2} + Z \\ X_3^t = 0.8X_3^{t-1} + N_{X_3} \\ X_4^t = 0.8X_2^{t-1} + N_{X_4} \end{cases} \quad (\text{B.6})$$

where $N_{X_n} \sim \mathcal{U}(0, 1)$. β is selected a number from the interval $[0.5, 3.0]$ with 0.2 step size. Z indicates the root cause factor that follows $Z = z$. The value of $Z = z$ at sample $T = 500$ is selected from the intervals $[0.0, 10]$ with 0.5 step, otherwise set as $Z = 0$.

The target anomalous sample for the model F_2 was generated in the same manner as that of the model F_1 by using the following models:

$$F_{2_{testA}} := \begin{cases} X_1^t = 0.2X_1^{t-1} + N_{X_1} + Z \\ X_2^t = \beta X_1^{t-1} + 0.4X_3^{t-1} + N_{X_2} \\ X_3^t = 0.2X_3^{t-1} + N_{X_3} \\ X_4^t = 0.1X_2^{t-1} + N_{X_4} \end{cases} \quad (\text{B.7})$$

$$F_{2_{testB}} := \begin{cases} X_1^t = 0.2X_1^{t-1} + N_{X_1} \\ X_2^t = 0.2X_1^{t-1} + 0.4X_3^{t-1} + N_{X_2} + Z \\ X_3^t = 0.2X_3^{t-1} + N_{X_3} \\ X_4^t = \beta X_2^{t-1} + N_{X_4} \end{cases} \quad (\text{B.8})$$

$$F_{2_{testC}} := \begin{cases} X_1^t = 0.2X_1^{t-1} + N_{X_1} \\ X_2^t = \beta X_1^{t-1} + 0.4X_3^{t-1} + N_{X_2} + Z \\ X_3^t = 0.2X_3^{t-1} + N_{X_3} \\ X_4^t = 0.1X_2^{t-1} + N_{X_4} \end{cases} \quad (\text{B.9})$$

B.2.2. ADDITIONAL RESULT: NON-TIME-SERIES CASE

In this section, we showed sensitivity analysis results similar to Section 3.2 for non-time-series cases. We generate training data from the following two linear models.

$$F_1^{appx} := \begin{cases} X_1 = N_{X_1} \\ X_2 = 0.8X_1 + 0.8X_3 + N_{X_2} \\ X_3 = N_{X_3} \\ X_4 = 0.8X_2 + N_{X_4} \end{cases} \quad (\text{B.10})$$

$$F_2^{appx} := \begin{cases} X_1 = N_{X_1} \\ X_2 = 0.2X_1 + 0.4X_3 + N_{X_2} \\ X_3 = N_{X_3} \\ X_4 = 0.1X_2 + N_{X_4} \end{cases} \quad (\text{B.11})$$

By applying the above models as the causal graph for evaluating RCA, we attempted to detect the root cause in the target outlier sample of each model. The target outlier sample for the model F_1^{appx} is generated by the following models:

$$F_{1_{testA}}^{appx} := \begin{cases} X_1 = N_{X_1} + Z \\ X_2 = \beta X_1 + 0.8X_3 + N_{X_2} \\ X_3 = N_{X_3} \\ X_4 = 0.8X_2 + N_{X_4} \end{cases} \quad (\text{B.12})$$

$$F_{1_{testB}}^{appx} := \begin{cases} X_1 = N_{X_1} \\ X_2 = 0.8X_1 + 0.8X_3 + N_{X_2} + Z \\ X_3 = N_{X_3} \\ X_4 = \beta X_2 + N_{X_4} \end{cases} \quad (\text{B.13})$$

$$F_{1_{testC}}^{appx} := \begin{cases} X_1 = N_{X_1} \\ X_2 = \beta X_1 + 0.8X_3 + N_{X_2} + Z \\ X_3 = N_{X_3} \\ X_4 = 0.8X_2 + N_{X_4} \end{cases} \quad (\text{B.14})$$

where $N_{X_n} \sim \mathcal{U}(0, 1)$. β and Z are the control variables for the causal mechanism changes and amplitude of root-cause noise, respectively. The value of each parameter is selected in the same manner as in Section 3.2. The outlier sample corresponding to F_2^{appx} is generated by the following

models:

$$F_{2_{testA}}^{appx} := \begin{cases} X_1 = N_{X_1} + Z \\ X_2 = \beta X_1 + 0.4X_3 + N_{X_2} \\ X_3 = N_{X_3} \\ X_4 = 0.1X_2 + N_{X_4} \end{cases} \quad (\text{B.15})$$

$$F_{2_{testB}}^{appx} := \begin{cases} X_1 = N_{X_1} \\ X_2 = 0.2X_1 + 0.4X_3 + N_{X_2} + Z \\ X_3 = N_{X_3} \\ X_4 = \beta X_2 + N_{X_4} \end{cases} \quad (\text{B.16})$$

$$F_{2_{testC}}^{appx} := \begin{cases} X_1 = N_{X_1} \\ X_2 = \beta X_1 + 0.4X_3 + N_{X_2} + Z \\ X_3 = N_{X_3} \\ X_4 = 0.1X_2 + N_{X_4} \end{cases} \quad (\text{B.17})$$

By using the above settings, the simulations of sensitivity analysis of RCA in non-time-series case were conducted with the same procedures as in the Section 3.2.

As shown in Fig. B.1, we found a similar tendency of the results as those of the time-series cases. This result suggested that, similar to the case of time-series data, the RCA in non-time-series case is also difficult to correctly detect the root cause Z when:

- the amplitude of the root cause Z is smaller than the background observational noise, or
- the root cause variable has no causal effect on the target variables.

B.3. Effects of sample sizes on CD-RCA

B.3.1. MODEL SETTINGS

As stated in the Section 3.3, the training data were generated by the following linear causal model:

$$F_{sim2}^{train} = \begin{cases} X_1^t = 0.8X_1^{t-1} + N_{X_1} \\ X_2^t = 3.8X_1^{t-1} + 0.8X_3^{t-1} + N_{X_2} \\ X_3^t = 0.8X_3^{t-1} + N_{X_3} \\ X_4^t = 3.8X_2^{t-1} + N_{X_4} \end{cases} \quad (\text{B.18})$$

where, $N_{X_n} \sim \mathcal{U}(0, 1)$. Note that X_4 is the target variable of the RCA. These generated data were applied to PCMCI-based causal graph estimation algorithm, and this estimated graph were applied as causal models for RCA in the target outlier sample.

The target outlier sample in this evaluation was generated with the following model:

$$F_{sim2}^{test} = \begin{cases} X_1^t = 0.8X_1^{t-1} + N_{X_1} + Z \\ X_2^t = 3.8X_1^{t-1} + 0.8X_3^{t-1} + N_{X_2} \\ X_3^t = 0.8X_3^{t-1} + N_{X_3} \\ X_4^t = 3.8X_2^{t-1} + N_{X_4} \end{cases} \quad (\text{B.19})$$

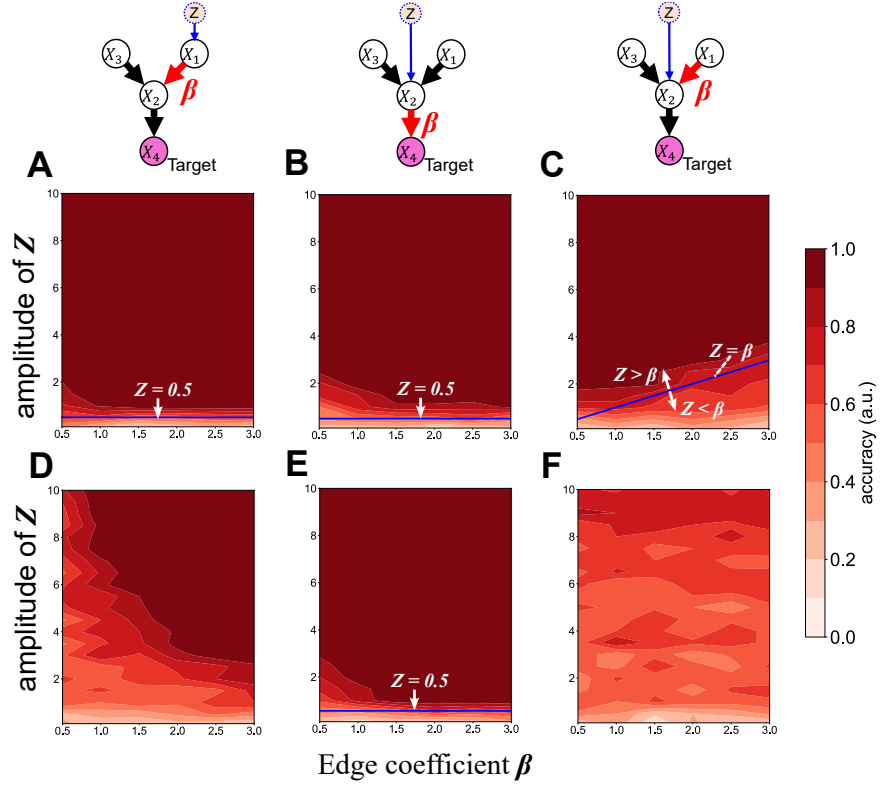


Figure B.1: **Additional result: sensitivity analysis of RCA for non-time-series data.** (A–C) The results of the root cause detection accuracy relative to the changes in amplitude of Z and graph edge weight β in the model F_1^{approx} . The causal graph diagrams of each panel indicates the location of the exact root-cause (Z) and edge changes (β) for each simulation settings. The lower three panels (D–F) The results of the model F_2^{approx} in the same manner of (A–C).

where $N_{X_n} \sim \mathcal{U}(0, 1)$. Z indicates the root cause variable. The value of Z was selected with the procedures described in Section 3.3. By using the above settings, the RCA analysis was conducted based on the following steps:

1. Generate training datasets \mathcal{D}_{train} with the causal models: F_{sim2}^{train} .
2. Estimate the time-series causal graph \mathcal{G} from the dataset \mathcal{D}_{train} with selected sample size N_{sample} using bootstrapping PCMC1.
3. Generate target outlier samples based on $\mathcal{F}_{sim2}^{test}$.
4. Apply the CD-RCA method to the target outlier sample with estimated causal graph \mathcal{G} (calculate the root-cause attributions $\phi(p)$ of each observational variables X_p).
5. Determine the root cause node based on the resulting value of $\phi(p)$ in Step 4.

6. Repeat 1–4 until accomplishing evaluation for all conditions of sample size N_{sample} in the Step 2.

Note that the causal graph \mathcal{G} was obtained from \mathcal{D}_{train} based on PCMCI with bootstrapping (Debeire et al., 2024) with 500 bootstrap samples. Due to randomness of this algorithm, the graph estimation with bootstrapping PCMCI was repeatedly conducted 10 times (i.e, 10 causal graphs were obtained for each time sample size condition N_{sample}). Therefore, 10 sets of attributions ϕ in Step 4 are calculated for each sample size.

B.4. Comparisons with baseline methods in non-time-series data

As mentioned in Section 3.4, the training data for learning the predictor f and the causal graph were generated by the following model:

$$F_{sim3}^{train} := \begin{cases} X_1 = N_{X_1} \\ X_2 = 3.8X_1 + 0.8X_3 + N_{X_2} \\ X_3 = N_{X_3} \\ X_4 = 3.8X_2 + N_{X_4} \end{cases} \quad (\text{B.20})$$

where $N_{X_n} \sim \mathcal{U}(0, 1)$. Note that X_4 is the prediction target of the ML model in this simulation.

Also, the target outlier samples for CD-RCA evaluation in this simulation were generated by the following model:

$$F_{sim3}^{test} := \begin{cases} X_1 = N_{X_1} + Z \\ X_2 = 3.8X_1 + 0.8X_3 + N_{X_2} \\ X_3 = N_{X_3} \\ X_4 = 3.8X_2 + N_{X_4} \end{cases} \quad (\text{B.21})$$

where $N_{X_n} \sim \mathcal{U}(0, 1)$ and Z indicated the observational noise and unobserved root cause variable, respectively.